Kimiabeigi M, Widmer J.

On Winding Design of a High Performance Ferrite Motor for Traction Application.

In: XXII International Conference on Electrical Machines (ICEM).

4-7 September 2016, Lausanne: IEEE.

DOI link to paper:

http://dx.doi.org/10.1109/ICELMACH.2016.7732790

Date deposited:

11/01/2017

On Winding Design of a High Performance Ferrite Motor for Traction Application

M. Kimiabeigi, J. D. Widmer

Abstract – **Design of low cost traction motors with ferrite magnets needs to meet challenges such as minimizing the risk of demagnetization, and maximizing the torque and power density, via a suitable choice of rotor and stator winding topology and parameters. With regards to the stator, distributed and concentrated windings may have both advantages and disadvantages when considering manufacturing cost, slot fill factor, the contribution factor of reluctance torque and parasitic effects. Furthermore, the trend toward high speed operation of the traction motors may increase the AC loss effects in the windings, contributing to motor deficiencies and risk of thermal failure. In this paper, the performance of a high speed ferrite motor with a distributed and concentrated wound stator, and with regards to torque and power performance as well AC loss effects is assessed. The dynamic performance of a full scale prototype design based on a distributed aluminum wound stator is presented.**

Index Terms—**AC Loss, Aluminum, Concentrated Winding, Distributed Winding, Ferrite, High Speed, Traction.**

I. Introduction

PERMANENT magnet motors with rare earth magnets are amongst the most popular candidates for traction applications, due to their high torque and power density, and efficiency, [1]-[6]. However, due to the high and unpredictable cost of the rare earth material, in particular Dysprosium which increase the demagnetization withstand capability of NdFeB magnets at high temperatures, [7], research toward using rare earth free designs, such as those with ferrite magnets have, recently, become popular, [8]-[14]. While different rotor topologies with ferrite magnets, including spoke type in [10], [11], [12], Multi-layer U and V shapes in [13], [14] and [15], and novel LC type in [16], have been reported, the majority are interior permanent magnet (IPM) type to exploit the reluctance torque, as well as reducing the risk of demagnetization via rotor core acting as a magnetic bypass, [12], [13].

With regards to the stator and windings, both concentrated (CW), [11], [16], and distributed (DW), [10], [12], [13], [14], [15], windings have been proposed, where the concentrated option reduces the costs (due to the simplicity of the manufacturing and possibility of stator modularity) at the cost of lower saliency and lower contribution from the reluctance torque. Furthermore, with a concentrated winding with modular stator core, a greater slot fill factor can be achieved, as a result of which the DC winding loss is mitigated and the power density may be enhanced, [17], [18]. Several papers have compared the performance of concentrated and distributed windings applied to IPM motors, amongst which most have addressed the extra core and magnet losses as well as acoustic noise and vibration due to the additional Magneto Motive Force (MMF) harmonics associated with the concentrated windings, [17], [19], [20]. In [21]-[24], the torque-speed performance of a distributed winding is reported to be superior to a concentrated winding in both constant torque and constant power region, due to the higher saliency ratio.

Another important aspect of traction motors, especially those with high top speed rating (to obtain a high power density and a high constant power speed ratio, CPSR) is to mitigate the AC losses in the windings. In [25], a one dimensional analytical model of the AC loss in a distributed winding has been proposed and proved with only 5% inaccuracies when compared against FE modelling. In [26], the proximity effect in several combinations of parallel and series wire connections and for a concentrated wound traction motor have been studied, and shown that without a transposition, [27], the losses in a bundle of parallel wires may concentrate in few individual wires, leading to hot spots and possible motor failure. In [28], the extra time harmonics due to PWM switching were shown to pronounce the proximity and skin effect losses, while in [29], a computationally efficient method to calculate skin and proximity losses with account for the temperature effects has been proposed.

Finally, the choice between star and delta connections for three phase windings might have implications on some parasitic effects related to flux 3rd order harmonics. In [30], it is shown that in an induction motor (IM) the 3rd harmonic flux due to the magnetic saturation may result in extra core losses, while it is commented that the delta connection might affect these losses via cancelation of the 3rd order harmonics. Furthermore, several papers have investigated the drive advantages via switching between star and delta connection, [31], [32], (due to the voltage per coil differences between the two connections). However, no paper has provided a comparison between the two winding connections in terms of AC losses.

In this paper, the performance of a high power density low cost ferrite motor, [12] and [33], with regards to the stator windings will be assessed. In this regard, the distributed wound stator is compared against a concentrated wound alternative, while the rotor in both cases is kept identical to the base line rotor design in [12]. First, for a limited DC voltage supply, the torque-speed performance of the motor, using the two alternative windings, is compared. Then, the AC winding losses for different scenarios including

This work is funded by Innovate UK under Grant 110130.

M. Kimiabeigi and J. D. Widmer are with Newcastle University, Newcastle Upon Tyne, NE17RU UK (e-mail: mohammad.kimiabeigi@ncl.ac.uk; james.widmer@ncl.ac.uk).

concentrated vs. distributed topology, different slot fill factor, random vs. organized wire lay-out, copper vs. aluminum, and star vs. delta connection have been evaluated. As a novel contribution of this paper, the significance of organized wire layout vs. random layout in terms of impact on AC losses is highlighted, while it is shown how maximizing the slot fill factor might, adversely, raise the AC losses in a winding. Furthermore, the advantage of using aluminum wires in terms of more balanced current distribution and lower risk of hot spot formation is, for the first time, demonstrated. Finally, the dynamic performance of a full scale prototype motor with ferrite magnets and aluminum windings has been measured and compared against the project requirements, as well as the Nissan Leaf 2010 design with rare earth magnets and copper windings.

II. Torque and Power Performance

The main requirements of a high speed ferrite motor, specified as part of an all-electric vehicle project, [12], [33], are summarized in Table I. Furthermore, a schematic of the stator and rotor geometry for both a distributed winding (with 2 slots per pole and phase) and a concentrated winding (with 0.5 slot per pole and phase) as well as some major dimensions are included in Fig. 1. and Table II. With regards to the design methodology, the following comments should be noted: a) the rotor geometry is a result of a coupled electromagnetic-structural optimization process which has been explained in [12], [33], b) the stator topology with the distributed winding is the result of an optimization to achieve maximum torque, and a minimum ripple torque, while the open rectangular slots were chosen to maximize the flux linkage and simplify coil insertions, c) the stator topology with the concentrated winding is the result of a manual optimization, to achieve a maximum torque while the outer and inner bore diameters were kept fixed and identical to the design with the distributed winding (this was to enable using the same rotor and the same stator housing for the two designs for a simpler comparison).

Table I
Design Requirements for the High Speed Ferrite Motor.

Gross volume (including cooling and end winding)	< 14 liter
Peak power density per motor volume	>6 kW/liter
Continuous power density per motor volume	>4 kW/liter
Base to top speed ratio	3000 rpm : 15000 rpm
Maximum winding temperature	180 °C
Available water cooling options	Only via outer stator frame
Demagnetization withstand capability	Against 3-phase short circuit
Ferrite, B_r at 20°C/ H_{cj} at -40°C	0.43 T/ 330 kA/m
Minimum available DC link voltage	400 V
Maximum peak inverter current	420 A

Table II
Major Dimensions of the High Speed Ferrite Motor.

Stator outer diameter (mm)	205
Rotor outer diameter (mm)	140
Stack length (mm)	195
Airgap (mm)	0.5

To evaluate the performance of the motor at base and top speed, a 2 dimensional Finite Element (2D FE) was used, where the drive was modelled using a sinusoidal current source with the maximum available line to line voltage fixed to the available DC link voltage of 400 V, Table I (assuming >100% inverter modulation index). The voltage and current waveforms for the two alternative windings at 3000 rpm and 15000 rpm, as well as the peak torque and power vs. speed curves for the entire speed range are shown in Figs. 2, 3 and 4, where U_{aN} and U_{ab} correspond to line to neutral and line to line voltages, respectively. To explain the findings, the direct (L_d), quadrature (L_q) axis inductances and saliency ratio (L_q/L_d) vs. the current have been calculated using FE 2D and the standard phasor diagram method in [34], (1) and (2), where v_d , i_d , v_q , and i_q are the d-axis and q-axis voltage and currents, λ_m is the magnet flux linkage, and r_s and ω_r are the winding resistance and rotor speed (rad/ sec), the results are shown in Fig. 5.

$$v_q = r_s \cdot i_q + w_r \cdot (L_d \cdot i_d + \lambda_m) \quad (1)$$

$$v_d = r_s \cdot i_d - w_r \cdot L_q \cdot i_q \quad (2)$$

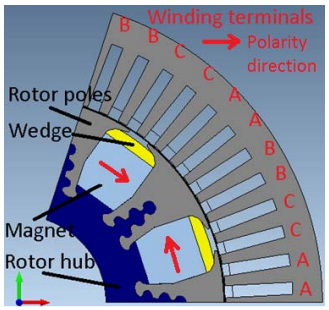

(a)

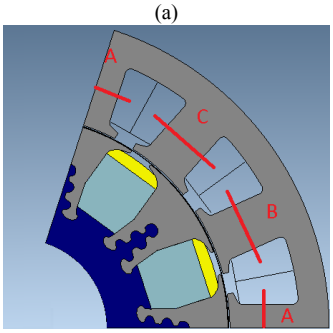

(b)

Fig.1. Schematics of high speed ferrite motor. (a) Distributed winding. (b) Concentrated winding.

From Figs. 2 to 5, it can be realized that: a) due to the higher per unit inductance associated with the concentrated winding (due to the additional Magneto Motive Force, MMF, harmonics), for a voltage limited application such as traction, the base speed is lower compared to the distributed winding, while for the speeds above the base speed, lower currents and, thereby, lower torque compared to distributed winding design, can be achieved, b) in the constant torque region, the concentrated winding design provides lower peak torque, due to the lower saliency ratio as well as lower winding factor, i.e. 86.6% vs. 96.6% for the distributed winding design, c) despite the lower peak power, the concentrated winding design may provide a competitive or, even, higher constant power speed ratio (CPSR) compared to

the distributed winding design; this is due to the larger per unit L_d (which enables the field weakening with lower available per unit current), as well as improvement of the concentrated winding design saliency by approaching the high speed-low current operating range due to the lower magnetic saturation, Fig. 5(b). Finally it should be noted that for the simulation results in Figs. 2 to 5, no rotor or stator skew has been assumed, which, in part, explains the significant harmonic contents in the voltage waveforms in Figs. 2 and 3.

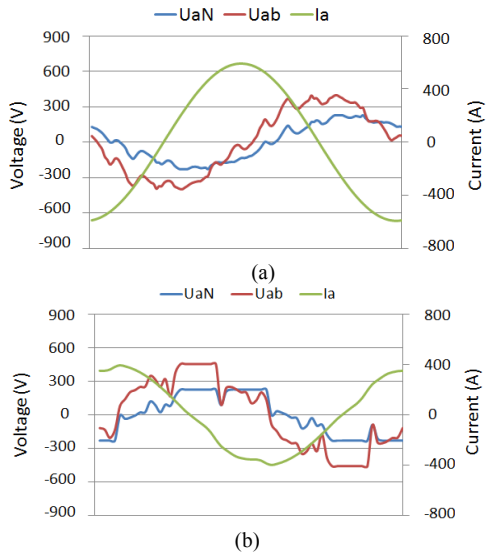

Fig. 2. Voltage and current waveforms at 3000 rpm rotor speed. (a) Distributed winding. (b) Concenrated winding.

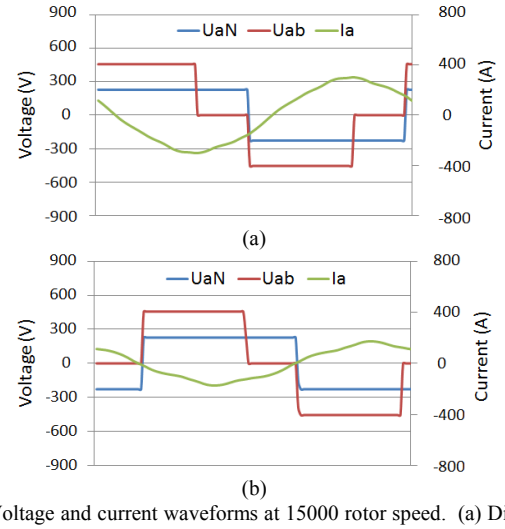

Fig. 3. Voltage and current waveforms at 15000 rotor speed. (a) Distributed winding. (b) Concenrated winding.

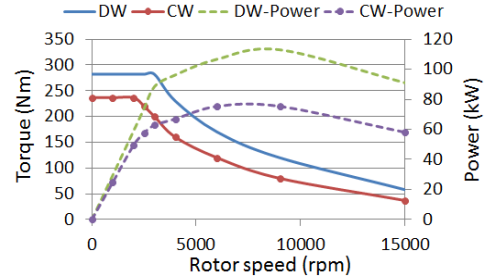

Fig. 4. Torque vs. speed for distributed against concentrated winding.

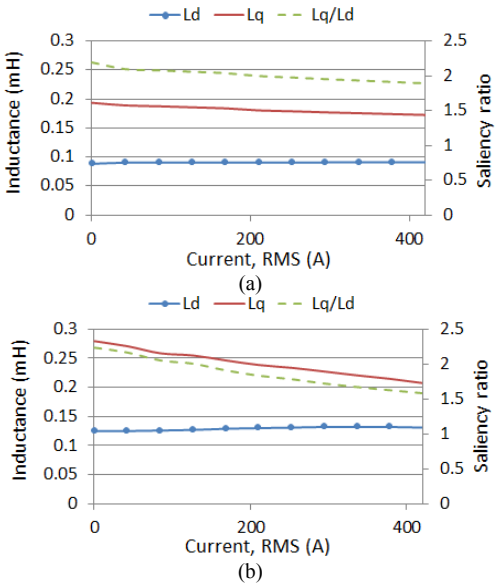

Fig. 5. D and Q-inductance and saliency ratio vs. current. (a) Distributed winding. (b) Concenrated winding.

III. Winding Losses

The winding losses, in a traction motor, constitute the majority of the total losses during the high torque low speed region, while they still may be comparable or larger than the iron losses during the low torque high speed region due to the losses associated with the field weakening current. Due to the high power density and large CPSR requirement of the traction motors, these motors are usually designed with a high top speed rating, such as the HSFM in this paper, as a result of which, care must be taken to avoid excessive AC losses in the windings.

By increasing the slot fill factor, defined as the conductor area to the total slot area, the DC winding losses can be reduced proportionally. On this basis, the concentrated winding with a modular stator is, usually, regarded as a higher efficiency option, due to the higher achievable fill factor compared to the distributed winding design. However, through the studies of the AC losses by the authors, it has been realized that if the additional fill factor results in a random lay out of the parallel wires, the AC losses might be pronounced to such an extent that lower fill factor options with an organized wire layout might be preferred. To demonstrate this effect in the current paper, the concentrated winding design in Section I is fitted with 16 turns and 6 wires in parallel per turn for a low fill factor option with an organized wire layout, Fig. 6(a), and with one additional wire per turn for a high fill factor option, where due to the additional wire, the disposition of the wires in the preferred layout becomes more complex to achieve, thereby a random layout has to be assumed, Figs. 6(b) and (c). It should be noted that by the organized layout, it is meant to maintain all or maximum number of the parallel wires within one turn in the same radial location; this is to minimize the dominant part of the proximity effects due to the dominant variation of the slot leakage flux in the radial direction compared to the circumferential direction. With regards to the random layout, two scenarios were assumed where the wires were disposed

once in the optimistic configuration, Fig. 6(b), i.e. most of the wires were accommodated in the same radial location to experience the least proximity effects, and once in the pessimistic configuration, Fig. 6(c), where most of the wires were disposed in different radial locations, to experience the largest proximity effects.

The time average winding loss distribution in the wires from the AC loss analysis in 2D FE (a transient motion analysis with the effects of the magnets included) have been shown in Fig. 7, and the total loss over DC loss factor in average and for the conductor with the largest losses have been summarized in Table III. Based on Fig. 7 and Table III the following comments can be made: a) when the parallel wires belonging to each turn are organized circumferentially, the losses are more uniformly distributed, thereby the AC loss factor is minimum, b) however, when the parallel wires are randomly distributed, the current density and losses tend to concentrate in the conductors which are located in the more inward radial locations, i.e. the locations with higher slot leakage ratio and, relatively, closer to the field variation from the magnets, c) as a result, and as indicated in Table III, not only may the quality of the wires disposition influence the average total winding losses, influencing the efficiency of the motor, but also it may result in severe formation of local hot spots in the winding, as in the pessimistic scenario the hot spot conductor may experience up to 64.2 times the average per wire DC loss.

With regards to aluminum wires, from Fig. 7 (d) and Table III, it can be realized that even though using aluminum instead of copper wires will raise the DC losses, it may, significantly, mitigate the AC loss effects. To explain the impact further, a summary of the DC and total loss values at base and top speed peak power operating points have been reported in Table IV, where cells indicating the maximum losses have been highlighted. From Table IV it is realized that, with regards to the maximum total loss, the copper winding results in 30% lower combined DC and AC losses compared to aluminum, which is less significant than 75% ratio when only DC losses are compared (due to 75% lower resistivity of copper). However, the main advantage of using aluminum is revealed when the local effects, i.e. the losses in the individual conductors are compared. In this respect, the maximum loss per aluminum conductor (indicated as worst conductor in Table IV), is about, only, 68% of the design with copper windings. Accounting for the non-ideal transfer heat coefficient between the wires (due to the insulations and air voids between the wires), the lower power losses in the individual conductors may result in lower risk of local hot spot formations, which may ultimately result in higher power capability and reliability of the designs based on the aluminum windings.

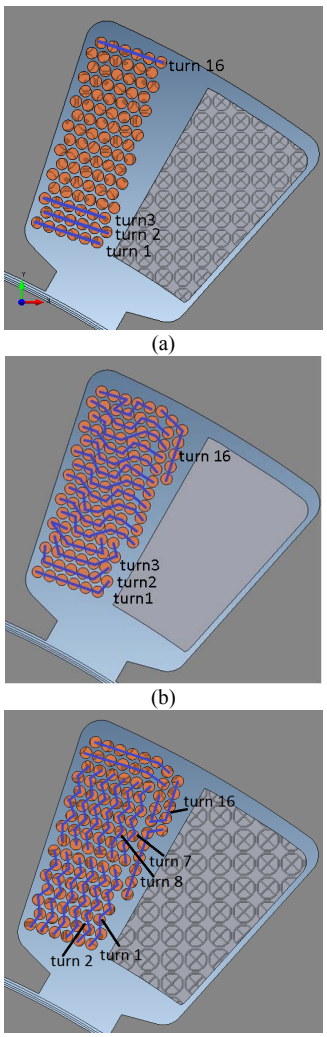

Fig. 6. The layout of turns and parallel wires in the concentrated winding design. (a) Organized layout with low fill factor. (b) Random layout with high fill factor, optimistic. (c) Random layout with high fill factor, pessmistic.

To assess the AC loss effect in a distributed winding design, the stator in Fig. 1(a) has been fitted with a 16 turn winding, with each turn composed of 3 parallel wires, Fig. 8(a). Due to the suitable fit of the slot aspect ratio to the specified number of turns and wires, it was estimated that the proposed wire layout was achievable in the manufacturing phase. From Table III, it can be realized that the proposed organized layout has resulted in a very low AC loss factor, which has been, further, enhanced by changing the wires from copper to aluminum. Furthermore, a comparison of the distributed against concentrated winding option reveals that the distributed design may result in lower AC loss effects, which can be attributed to the lower per unit slot leakage flux in the case of distributed winding design. Finally, a comparison of the Star and Delta connection has been made, where a delta connected 28 turn distributed winding with 6 parallel wires per turn organized in a preferred layout has been analyzed, Fig. 8(b) and Table III. The voltage and current drive of the Delta connected design has, furthermore, been adjusted so that a similar torque and power performance as that with the Star winding could be achieved.

Based on the results in Table III, it was realized that due to the smaller wire size (as a result of the higher number of turns) in a Delta connected design, lower AC losses can be achieved. However, this conclusion is, only, valid, when assuming that the parallel wires can, still, be disposed in a preferred lay-out, since a random lay-out of the wires may negate the effect of the smaller wires and raise the AC losses significantly.

TABLE III
AVERAGE AND WORST CONDUCTOR AC LOSS FACTOR FOR CW AND DW DESIGNS WITH DIFFERENT WIRE LAYOUTS AND MATERIALS.

	AC+DC/DC, total	AC+DC/DC, worst conductor
CW, Copper, Random-Pessimistic lay-out	7.9	64.2
CW, Copper, Random-Optimistic lay-out	2.3	11.7
CW, Aluminum, Random-Optimistic lay-out	1.5	4.6
CW, Copper, Organized lay-out	1.6	8.1
DW, Copper, Organized lay-out	1.4	5.8
DW, Aluminum, Organized lay-out	1.1	3.0
DW, Aluminum, Organized lay-out, DELTA	1.02	1.3

TABLE IV
COMPARISON OF ALUMINUM AND COPPER WINDING LOSS, CW RANDOM-OPTIMISTIC LAY-OUT, AT 2 KRPM AND 15 KRPM.

	Copper, total (W)	Aluminium, total (W)	Copper, worst conductor (W)	Aluminium worst conductor (W)
3 krpm, DC loss	3800	6500	33.9	58
3 krpm, AC+DC loss	4500	6900	82.3	85.8
15 krpm, DC loss	2060	3600	18.4	32.1
15 krpm, AC+DC loss	4800	5300	215.3	146.7

IV. PROTOTYPE TESTING

The HSFM design with the aluminum distributed winding according to Figs. 1(a) and 8(a) (a disposition of the parallel wires close to the ideal pattern in Fig. 8(a) was achieved during the manufacturing) was manufactured and subjected to a dynamic performance testing, Fig. 9. The intermittent and continuous performance from an initial rotor temperature of 65 ˚C was measured at different rotor speeds, and under 400 V DC link voltage. The temperature rise as well as current and torque response for the 3000 rpm are shown in Fig. 10(a), and the torque-power performance for the entire speed range and the comparison against the requirements are shown in Fig. 10(b). The preference of aluminum over copper windings for the prototype motor, despite the aluminum higher total losses in Table IV, is, primarily, to assess the reliability of this rather uncommon concept in a high power density traction application. Furthermore, the choice of aluminum wires resulted in a ~70% winding mass saving (~ 5 kg), as well as a ~90% reduction of the windings cost, both due to the lower mass density, as well as the lower price of the aluminum compared to the copper, [37].

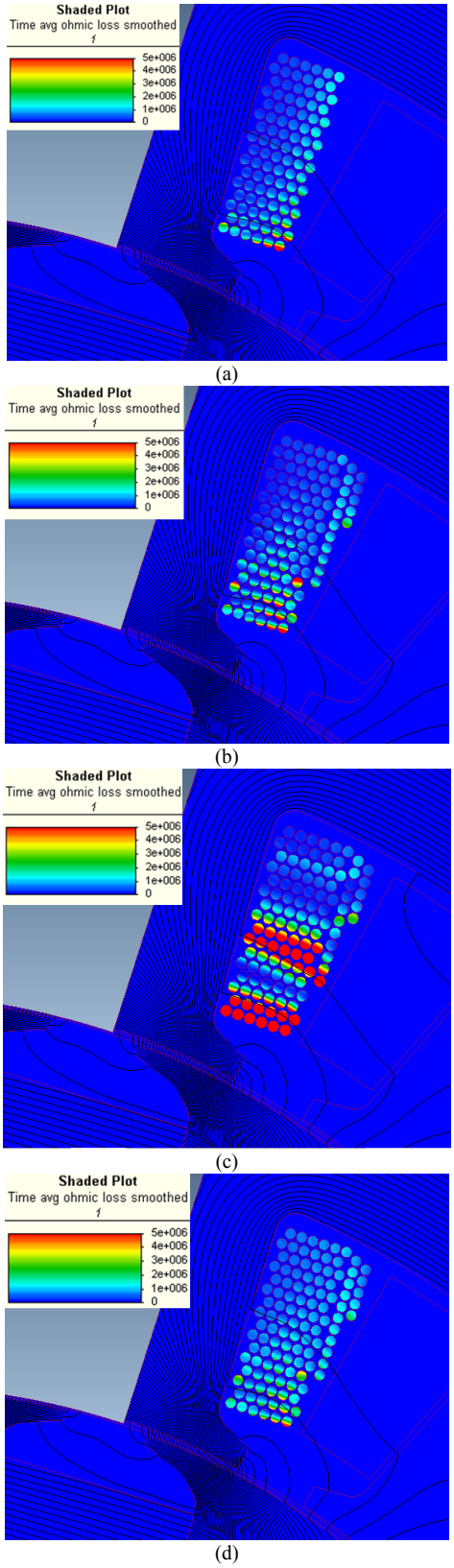

Fig. 7. Ohmic loss distribution and AC loss effects. (a) Organized layout. (b) Random layout, optimistic. (d) Random layout, Pessimistic. (d) Random layout, optimistic, Aluminium wires.

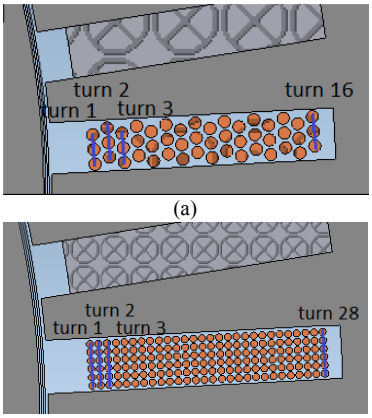

Fig. 8. The layout of turns and parallel wires in the distributed winding design. (a) Organized layout, STAR. (b) Organized layout, DELTA.

From Figs. 10(a), it can be realized that the HSFM design with the aluminum windings is capable of providing the maximum torque and power for a duration of about 30 seconds, which exceeds the requirement of 10 seconds and matches well with the initial thermal assessments of the dummy stator set up in [35]. From Fig. 10(b), it is realized that even though the HSFM design provides about 10% lower peak torque compared to the requirement, it, notably, provides a 24% higher peak power at a higher base speed. Furthermore, in terms of the continuous performance, even though the HSFM lags behind the required continuous power at lower speeds (due to the lower than required continuous torque at low speeds), it exceeds the continuous power requirement at the speeds above 6500 rpm, and provides a maximum continuous power of 60 kW, exceeding the requirement by 28%. Based on the results from the dynamic performance testing, it can be realized that the HSFM design with a distributed aluminum winding in the current paper (with 14 liter gross volume identical to the Leaf design), and with the rotor design disclosed in [12] and [33], may provide a competitive maximum torque and power density of 17 Nm/ liter (about 85% of the Leaf motor rating) and 6.4 kW/ liter (about 110% of the Leaf motor rating), and a maximum continuous power density of 4.3 kW/ liter (about 75% of the Leaf motor actual capability tested in [36]).

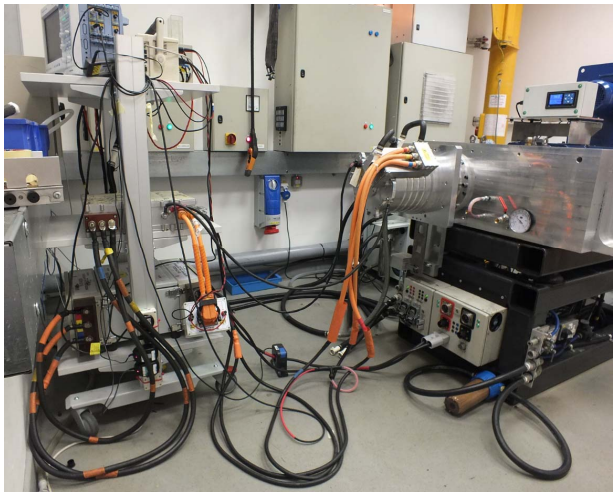

Fig. 9. Dynamic testing set up of the HSFM prototype.

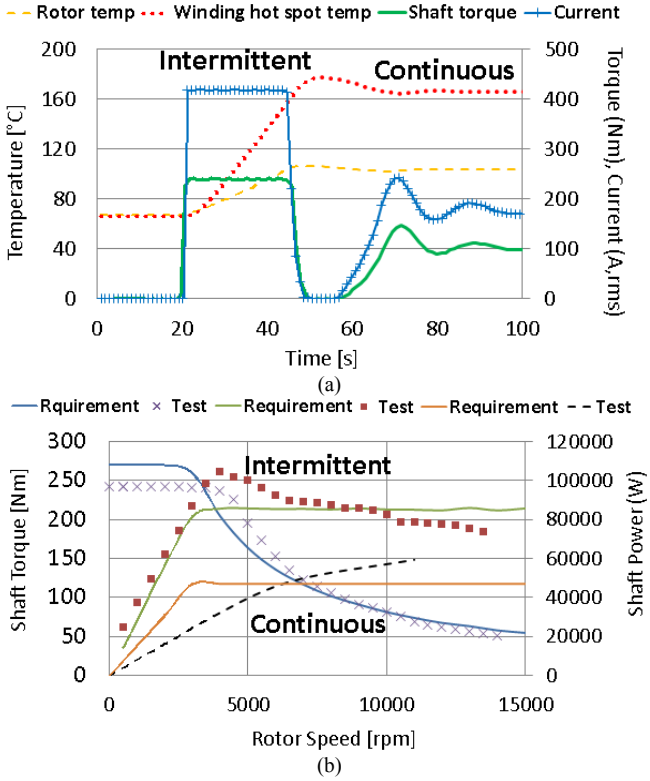

Fig. 10. Intermittent and continuous performance of the HSFM prototype under 400 V DC link voltage. (a) At 3000 rpm. (b) Test vs. requirement performance for the entire speed range.

V. Conclusions

The superiority of a distributed wound stator to a concentrated alternative in terms of higher torque and power density performance, and based on theoretical analyses, was demonstrated. It was shown that a distributed winding may benefit from a higher achievable current per unit DC link available voltage compared to a concentrated winding, due to the lower per unit inductance, while higher winding factor and saliency ratio in the former may result in a larger torque and power density of the motor. With regards to the AC loss effects, it was shown that the layout of the parallel wires within a turn can have a significant influence on the proximity losses. Furthermore, it was proposed and demonstrated that a suitable choice of the winding turns and parallel wires per turn may enable the designers to mitigate the AC losses via an organized disposition of the parallel wires in an ideal circumferential arrangement. Based on a comparison of aluminum against copper windings, the important benefit of using aluminum wires in mitigating the total losses in the individual conductors, thereby, reducing the risk of thermal failure due to the local hot spot formation was, for the first time, reported. In this paper, for the first time, the dynamic performance of a full scale prototype traction motor using low cost ferrite magnets and aluminum windings has been reported, and the prototype motor was shown to provide a highly competitive intermittent and continuous performance which, closely, matches the state of the art designs with rare earth magnets and copper windings. More specific prototype testing with regards to the AC losses and evaluation of the locally occurring hot spots is the scope of a future work.

VI. ACKNOWLEDGMENT

The authors acknowledge the support from Jaguar Land Rover and Continental Engineering under Evoque-E project.

VII. REFERENCES

[1] J. D. Santiago, H. Bernhoff, B. Ekergårdet, *et al*., "Electrical Motor Drivelines in Commercial All Electric Vehicles: a Review'', IEEE Trans. Vehicular. Tech., vol. 61, no. 2, pp 475-484, Feb. 2012.

[2] T. A. Burress, S. L. Campbell, C. L. Coomer, *et al*., "Evaluation of the 2010 Toyota Prius Hybrid Synergy Drive System,'' Oak Ridge Nat. Lab., Oak Ridge, TN, USA, ORNL/TM-2010/253, Mar. 2011.

[3] R. H. Staunton, T.A. Burress, and L.D. Marlino, "Evaluation of 2005 Honda Accord Hybrid Electric Drive System,'', Oak Ridge Nat. Lab., Oak Ridge, TN, USA, ORNL/TM-2006/535, Sep. 2006

[4] Y. Sato, S. Ishikawa, T. Okubo, et al., "Development of High Response Motor and Inverter System for the Nissan leaf electric Vehicle'', SAE Technical Paper 2011-01-0350, Apr. 2011.

[5] S. Jurkovic, K. Rahman, B. Bae, N. Patel, and P. Savagian, "Next generation chevy volt electric machines; design, optimization and control for performance and rare-earth mitigation" IEEE Energy Conversion Congress and Exposition (ECCE), Sep. 2015, pp. 5219 - 5226.

[6] Electrical drive motor for a vehicle, by J. Merwerth, J.Halbedel, and G. Schlangen. (2012, Oct). Patent US 2012/0267977.

[7] M. Komuro, Y. Satsu, and H. Suzuki, "Increase of coercivity and composition distribution in fluoride-diffused NdFeB sintered magnets treated by fluoride solutions," IEEE Trans. Magn., vol. 46, no. 11, pp.3831–3833, Nov. 2010.

[8] D.Dorrell, L.Parsa, and I.Boldea, "Automotive Electric Motors, Generators, and Actuator Drive Systems With Reduced or No Permanent Magnets and Innovative Design Concepts," IEEE Transactions On Indus Elects, Vol. 61, No. 10, pp 5693 - 5695, Oct 2014.

[9] J. D. Widmer, R. Martin, and M. Kimiabeigi, "Electric vehicle traction motors without rare earth magnets," Sustainable Materials and Technologies (Elsevier), Feb 2015.

[10] J. Galioto, P. B. Reddy, A. M. EL-Refaie, "Effect of Magnet Types on Performance of High Speed Spoke Interior Permanent Magnet Machines Designed for Traction Applications," in Proc. Energy Conversion Congress and Exposition (ECCE), Sep 2014, pp. 4513 - 4522.

[11] Y. Burkhardt, A. Spagnolo, P. Lucas, M. Zavesky, P. Brockerhoff, "Design and analysis of a highly integrated 9-phase drivetrain for EV applications," International Conference on Electrical Machines and Systems (ICEMS), Sep 2014, pp. 450 – 456.

[12] M. Kimiabeigi, J. D. Widmer, R. Long, Y. Gao, J. Goss, R. Martin, T. Lisle, J.M. Soler Vizan, A. Michaelides, and B. Mecrow, "High Performance Low Cost Electric Motor for Electric Vehicles Using Ferrite Magnets," IEEE Trans. Ind. Electron., vol. 63, no. 1, pp.113-122, Jan 2016.

[13] S. Morimoto, S. Ooi, Y. Inoue, and M. Sanada, "Experimental Evaluation of a Rare-Earth-Free PMASynRM With Ferrite Magnets for Automotive Applications,'' IEEE Trans. Ind. Electron., vol. 61, no. 10, Oct. 2014.

[14] B. Boazzo, A. Vagati, G. Pellegrino, E. Armando, and P. Guglielmi, "Multipolar Ferrite-Assisted Synchronous Reluctance Machines: A general design approach," IEEE Trans. Ind. Electron., vol. 62, no. 2, pp. 832-845, Feb. 2015.

[15] H. Cai, B. Guan, and L. Xu, "Low-cost ferrite PM-assisted synchronous reluctance machine for electric vehicles," IEEE Trans. Ind. Electron., vol. 61, no.10, pp.5741-5748, Oct. 2014.

[16] H. J. Kim, D. Y. Kim, and J. P. Hong, "Structure of Concentrated-Flux-Type Interior Permanent-Magnet Synchronous Motors Using Ferrite Permanent Magnets," IEEE Trans. Magn., vol. 50, no. 11, pp.113-122, Nov 2014, Art. ID 8206704.

[17] A. M. EL-Refaie, "Fractional-slot concentrated-windings synchronous permanent magnet machines: Opportunities and challenges," IEEE Trans. Ind. Electron., vol. 57, no. 1, pp. 107–121, Jan. 1, 2010.

[18] J. Widmer, R. Martin, B. Mecrow, "Pre-compressed and stranded aluminum motor windings for traction motors", Early access articles IEEE Trans. Ind. Appl, Feb 2016.

[19] F. Magnussen and H. Lendenmann, "Parasitic effects in PM machines with concentrated windings," IEEE Trans. Ind. Appl., vol. 43, no. 5, pp. 1223–1232, Sep./Oct. 2007.

[20] O. Bottauscio, G. Pellegrino, P. Guglielmi, M. Chiampi, and A. Vagati "Rotor loss estimation in permanent magnet machines with concentrated windings," IEEE Trans. Magn, vol. 41, no. 10, pp. 3913-3915, Oct. 2005.

[21] Y.Honda, T.Nakamura, T.Higaki, Y.Takeda, "Motor design considerations and test results of an interior permanent magnet synchronous motor for electric vehicles", hirty-second IAS Annual Meeting, 1997,Vol.1, pp.75-82.

[22] 1. 1. Lee, W. H. Kim, 1. S. Yu, S . Y. Yun, S. M. Kim, and 1. Lee, "Comparison between concentrated and distributed winding in IPMSM for traction application, " the international conference on electrical machines and systems (ICEMS), 2010, pp. 1172-1174.

[23] L. Chong , R. Dutta, N. Q. Dai, M. F. Rahman, H. Lovatt, "Comparison of Concentrated and Distributed Windings in an IPM Machine for Field Weakening Applications," Australasian universities Power Engineering Conference (AUPEC), Dec 2010, pp 1-5.

[24] S.-O. Kwon, S.-I. Kim, P. Zhang, and J.-P. Hong, "Performance comparison of IPMSM with distributed and concentrated windings," in 41st Conf. Rec. IEEE IAS Annu. Meeting, Oct. 8–12, 2006, vol. 4, pp. 1984–1988.

[25] H. Hamalainen, J. Pyrhonen, and J. Nerg, "AC Resistance factor in one layer form-wound winding used in rotating electrical machines," IEEE Trans. Magn., vol. 49, no. 6, pp. 2967–2973, Jun. 2013.

[26] M. Popescu and D. G. Dorrell, "Proximity losses in the windings of high speed brushless permanent magnet AC motors with single tooth windings and parallel paths," IEEE Trans. Magn., vol. 49, no. 7, pp. 3913–3916, Jul. 2013.

[27] P. B. Reddy, T. M. Jahns, and T. P. Bohn, "Transposition effects on bundle proximity losses in high-speed PM machines," in IEEE Energy Conversion Congress and Exposition (ECCE2009), 2009, pp.1919–1926.

[28] S. Iwasaki, R. Deodhar, Y. Liu, A. Pride, Z.Q. Zhu, and J. Bremner, "Influence of PWM on the proximity loss in permanent magnet brushless AC machines," IEEE Trans. Industry Applications, vol.45, no.4, pp.1359-1367, 2009.

[29] P. Mellor, R. Wrobel, and N. Simpson, "AC losses in high frequency electrical machine windings formed from large section conductors," in *Proc. IEEE Energy Convers. Congr. Expo. (ECCE)*, 2014, pp. 5563–5570.

[30] J.S. Hsu, H.P. Liou, B.T. Lin, W.F. Weldon, "losses influenced by third-harmonic flux in induction motors," vol. 6, no. 3, pp. 461- 468, Sep 1991.

[31] M. M. Swamy, T. Kume, A. Maemura, and S. Morimoto, "Extended high speed operation via electronic winding change method for AC motors," IEEE Trans. Ind. Appl., vol. 42, no. 3, pp. 742–752, May/Jun. 2006.

[32] S. Sadeghi, L. Guo, H. Toliyat, and L. Parsa, "Wide operational speed range of five-phase permanent magnet machines by using different stator winding configurations," IEEE Trans. Ind. Electron., vol. 59, no. 6, pp. 2621–2631, Jun. 2012.

[33] M. Kimiabeigi, J. D. Widmer, R. Long, Y. Gao, J. Goss, R. Martin, T. Lisle, J.M. Soler Vizan, A. Michaelides, and B. Mecrow, "On Selection of Rotor Support Material for a Ferrite Magnet Spoke Type Traction Motor," Accepted to be published in IEEE Trans. Ind. Appl.,Oct 2015.

[34] T. Sun, S.-O. Kwon, S.-H. Lee, and J.-P. Hong, "Investigation and comparison of inductance calculation methods in interior permanent magnet synchronous motors," in International Conference on Electrical Machines and Systems (ICEMS), 2008, pp. 3131–3136.

[35] M. Kimiabeigi, J. D. Widmer, R. S. Sheridan, A. Walton, R. Harris, "Design of high performance traction motors using cheaper grade of materials," accepted for presentation in 8th IET Int. Conf. Power Electron. Mach. Drives (PEMD 2016).

[36] S. A. Rogers, "Annual Progress Report Advanced Power Electronics and Electric Motors Program," US department of energy report, Jan 2013.[Online],Available:http://energy.gov/sites/prod/files/2014/04/f15/2013_apeem_report.pdf.

[37] London exchange market. [Online], Available: https://www.lme.com/.

VIII. BIOGRAPHIES

Mohammad Kimiabeigi received the M.S degree in electric power engineering from Royal Institute of Technology, Sweden, in 2008, and is currently working toward PhD at Newcastle University, UK. He has been a research engineer at ABB competence center, Sweden, Siemens Wind Power, Denmark, and Siemens Wind Power competence center, UK. Mr Kimiabeigi holds 12 granted European and U.S patents, 20 filed patent applications, and more than 10 journal and peer reviewed conference publications. During his career, he has been a lead design engineer for industrial and R&D projects in excess of £10 M.

James D. Widmer has a PhD in the design of electrical machines from Newcastle University, U.K. He joined Newcastle University in 2009 from a senior post in the aerospace industry. He is responsible for the "Centre for Advanced Electrical Drives," Newcastle University which works with industry partners to convert academic research into world-class products. His research interests include high-efficiency permanent magnet machines and rare-earth magnet-free motor topologies.